Feng *et al. Biochar* (2023) 5:53
https://doi.org/10.1007/s42773-023-00253-7

Biochar

ORIGINAL RESEARCH

Open Access

Geo-environmental and mechanical behaviors of As(V) and Cd(II) co-contaminated soils stabilized by goethite nanoparticles modified biochar

Chen Feng[1,2,3], Jiangshan Li[1,3,4*], Wenhao Jiang[1,2,3], Jindu Liu[1,2,3] and Qiang Xue[1,3*]

Abstract

Goethite nanoparticles modified biochar (FBC) could address the weak effectiveness of conventional biochar commonly to process heavy metal(loids) (HMs) co-contamination with different charges. However, few studies have focused on the change of soil mechanical properties after stabilization. In this study, FBC was synthesized to stabilize simultaneously arsenic (As (V)) (anions) and cadmium (Cd (II)) (cations) in co-contaminated soils. Batch adsorption, leaching toxicity, geotechnical properties and micro-spectroscopic tests were comprehensively adopted to investigate the stabilization mechanism. The results showed that FBC could immobilize As (V) mainly through redox and surface precipitation while stabilizing Cd (II) by electrostatic attraction and complexation, causing soil agglomeration and ultimately making rougher surface and stronger sliding friction of contaminated soils. The maximum adsorption capacity of FBC for As (V) and Cd (II) was 31.96 mg g^{-1} and 129.31 mg g^{-1}, respectively. Besides, the dosages of FBC required in contaminated soils generally were approximately 57% higher than those in contaminated water. FBC promoted the formation of small macroaggregates (0.25–2 mm) and the shear strengths of co-contaminated soils by 21.40% and 8.34%, respectively. Furthermore, the soil reutilization level was significantly improved from 0.14–0.46 to 0.76–0.83 after FBC stabilization according to TOPSIS method (i.e., technique for order preference by similarity to an ideal solution). These findings confirm the potential of FBC in immobilizing As (V) and Cd (II) of co-contaminated soils and provide a useful reference for green stabilization and remediation of HMs co-contaminated sites.

Highlights

- Goethite nanoparticles modified biochar (FBC) can make up the shortcoming of conventional biochar to immobilize simultaneously arsenic (As (V)) and cadmium (Cd (II)) in co-contaminated soils.
- FBC is conducive to the formation of the soil small macroaggregates (i.e., 0.25–2 mm).
- FBC promotes soil shear strengths of As (V) and Cd (II) co-contaminated soils by increasing internal friction.

Handling editor: Nabeel Khan Niazi

*Correspondence:
Jiangshan Li
jsli@whrsm.ac.cn
Qiang Xue
qxue@whrsm.ac.cn
Full list of author information is available at the end of the article

Keywords Arsenic, Cadmium, Co-contaminated soils, Goethite nanoparticles modified biochar, Stabilization, TOPSIS method

Graphical Abstract

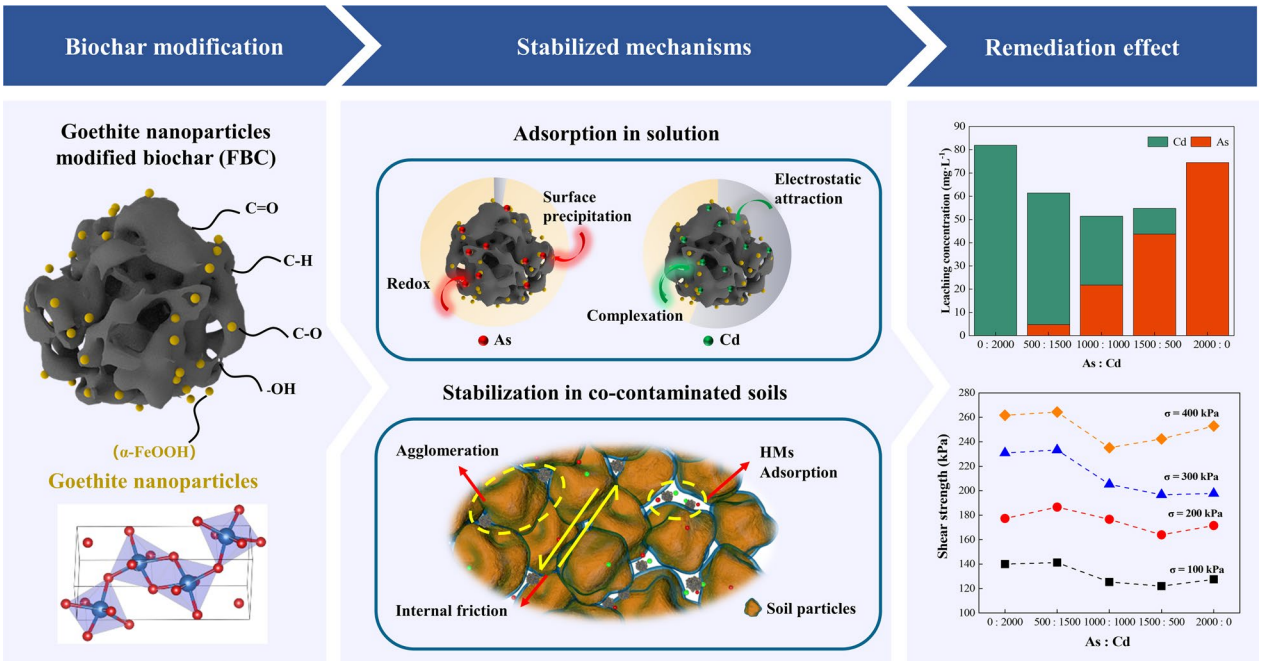

1 Introduction

Heavy metal(loid)s (HMs) contamination degrades the soil properties including the bio-availability, general stability, and soil strength, triggering failure disasters in the long term (Fan and Zhang 2018; Lin et al. 2020; Li et al. 2021). In China, the proportion of soil exceeding the environmental standard reached 16.1%, of which about 500,000 were contaminated sites of more than 10,000 m^2 (Xue et al. 2020), and the investment in soil remediation was about 15.66 billion yuan in the year 2021. Specifically, Arsenic (As) and Cadmium (Cd), as two priority HMs pollutants, mainly distribute in middle and upper reaches of the Yangtze River areas by co-contamination with a maximum HMs concentration of 7958 mg kg^{-1}, exceeding the standard limit by 56 times (Yang et al. 2018). Consequently, it is urgent to develop a green and efficient technique for simultaneously treating As and Cd co-contamination in soils.

Biochar (BC), as a green-stabilizer, has attracted increasing attention for remediation of contaminated soils and water for its high efficiency and low cost in recent decades (Xu et al. 2018; Wang et al. 2021; Zhou et al. 2022). BC has a good adsorption capacity for cationic HMs pollutants owing to its rich functional groups and abundant pore structure (Xu et al. 2018; Fan et al. 2020; Wang et al. 2022) But BC commonly shows little effect on anionic contaminations as the electronegativity of surface (Vithanage et al. 2017). For the target HMs in this study. As exists in the form of is anion groups (AsO_2^-, AsO_4^{3-}, $HAsO_4^{2-}$) while Cd exists in the form of cations (Cd^{2+}) (Takeno 2005), which leaves BC unable to satisfy simultaneous remediation of As and Cd co-contaminated soils. Goethite (α-FeOOH) nanoparticles (NPs) exhibited excellent adsorption capac

ity for both As and Cd by their great reactivity (Faria et al. 2014; Vinh et al. 2019). Nevertheless, they were difficult to directly apply in environmental engineering for their ultrafine nature and easy hardening in soil. The α-FeOOH NPs loaded BC can not only realize the remediation of As and Cd, but also ensure the uniform distribution and effectiveness in soils (Zhu et al. 2020b; Wan et al. 2022).

Goethite modified BC also has been employed in agricultural research to solve the environmental problem (Abdelrhman et al. 2022; Irshad et al. 2022). Abdelrhman et al. (2022) reported the goethite modified BC reduced Cd and As uptake by Chinese cabbage shoots

and roots through pot studies in co-contaminated paddy soil. The application of goethite modified biochar in soil showed promising results for the immobilization of both Cd and As (Zhu et al. 2020b). However, few studies have focused on the change of soil mechanical properties in As and Cd co-contaminated soils stabilized by goethite modified BC, which is important for geotechnical engineering. Conventional BC has confirmed decreasing effect on the compressibility of clayey soils (Zhang et al. 2020), the maximum dry density and shear strength (Ganesan et al. 2020). Therefore, the change in mechanical properties of As and Cd co-contaminated soils treated by goethite modified BC needs further exploration to make up for blanks.

In this study, we propose a green, sustainable, and low-cost multifunctional adsorbent goethite NPs modified BC (FBC) through co-precipitation method for stabilization of both As (V) and Cd (II) co-contaminated clayey soils. The specific objectives of this study are to: (1) clarify adsorption effect of FBC on As (V) and Cd (II) for both solution and co-contaminated soils; (2) explore the leaching toxicity and geotechnical properties of the stabilized soils; (3) investigate the corresponding stabilization mechanism; and (4) evaluate the soil reusability after treatment via the evaluation of technique for order preference by similarity to an ideal solution (TOPSIS) method.

2 Materials and methods

2.1 Preparation of goethite NPs modified biochar

2.1.1 Preparation procedure

The scheme to prepare the goethite NPs modified biochar (denoted as FBC) is graphically described in Fig. 1. At first, the corn straws were washed with pure water and dried in the oven. The tube furnace was fed N_2 for 0.5 h to provide an oxygen-free environment. Then the corn straws prepared above were placed into it and the pyrolysis temperature was set to 500 °C at a heating rate of 5 °C min^{-1}, followed by holding of 2 h. Afterwards, the residual solids were washed to obtain BC. After that, the BC was immersed into 5 mol L^{-1} KOH solution, the volume of which was fixed to 1 L by adding 1 mol L^{-1} $FeCl_3$ solution (Schwertmann and Cornell 2000). The mixes were subsequently agitated at 70 °C for 60 h. The polyethylene container, instead of normal glass beaker, was carried out in the whole process to prevent silicate melting under strong alkali conditions. Finally, the separated solids were repeatedly rinsed by pure water and dried at 60 °C to acquire FBC.

2.1.2 Characterization of FBC

The different surface functional groups and crystal mineral composition of BC and FBC are shown in Fig. 2. The bend vibration of ferrite bond (Fe–O) (580 cm^{-1}) hydroxyl group (–OH) (3308 cm^{-1}) and bond in the functional group (Zhu et al. 2020a, b), as well as new diffraction goethite peaks (PDF# 29–0713) (2θ = 21.08° and 39.62°), confirmed the goethite NPs were successfully loaded onto BC. The porous structures and different forms can be observed in Fig. 2c–e. Compared with unmodified BC, goethite NPs were uniformly distributed on the surface of BC to enlarge the specific surface area (SSA). To determine chemical and biodegradation of BC, elemental analysis was conducted (Table 1). The H/C and O/C ratio of FBC was slightly higher than that of BC, suggesting that the FBC was more beneficial to the long-term stabilization in soil.

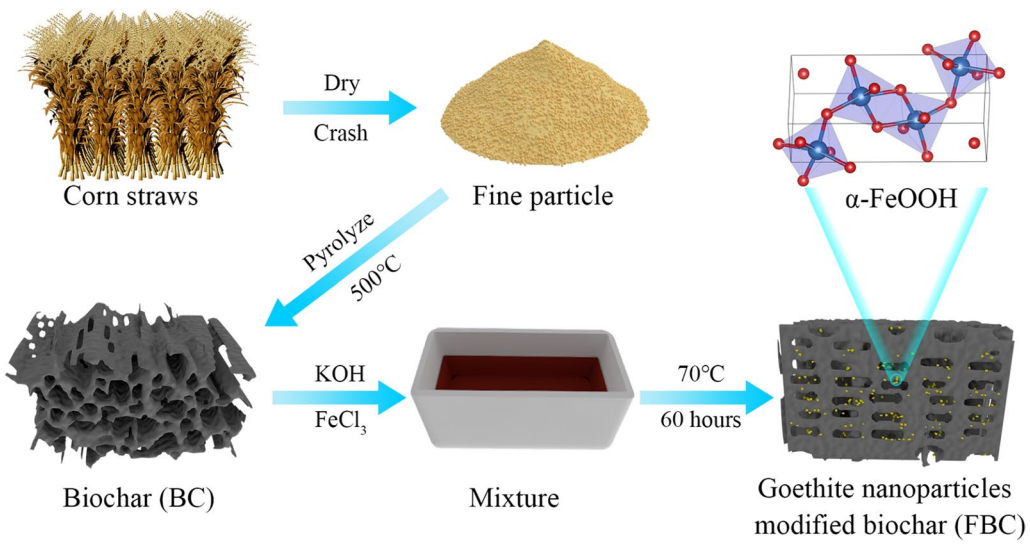

Fig. 1 The preparation procedure of goethite nanoparticles modified biochar

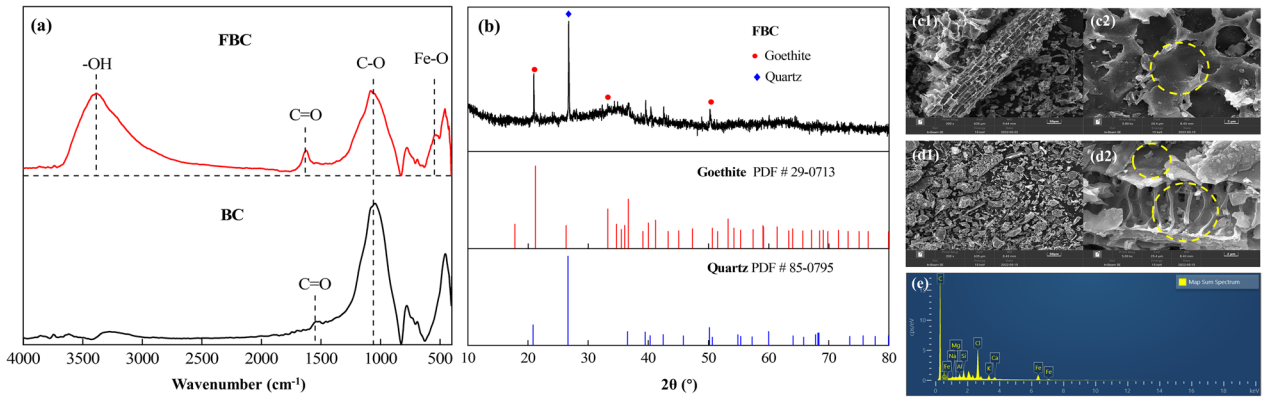

Fig. 2 Spectroscopic characterization of FBC: **a** FTIR spectrum; **b** XRD pattern; **c**–**e** SEM images and EDS analysis ((**c**) BC of 500_ magnifications (**c1**) and 5000_ magnifications (**c2**), (**d**) FBC of 500_ magnifications (**d1**) and 5000_ magnifications (**d2**), and (**e**) EDS of FBC in (**d2**))

Table 1 Main elemental composition and physical properties of BC and FBC

Specimen	C (%)	H (%)	O (%)	Fe (%)	pH	D_{10} (μm)	D_{50} (μm)	D_{90} (μm)
BC	53.68	0.75	8.36	–	8.82	19.4	100	462
FBC	46.19	0.81	12.82	9.14	9.17	61.7	287	831

2.2 Preparation of co-contaminated soils

Considering the extensive and heterogeneous sources of HMs contaminated soils, the co-contaminated soils of As (V) and Cd (II) were prepared in the laboratory to investigate the stabilization effect, and similar methods have been used in previous studies (Mohammad et al. 2020; Zhu et al. 2022). The raw soil was collected from the excavation for construction in Wuhan, China (30° 52' N, 114° 31' E). After passing 2 mm sieve, the raw soil was dried to constant weight in the oven at the temperature of 105 °C and deposited in a sealed plastic drum for the experiments. The basic geotechnical properties of the raw soil are in Table 2. For the co-contaminated soils, five groups were set up with a total contaminant concentration of 2000 mg kg^{-1}, but different proportions of As (V) and Cd (II). The As (mg kg^{-1}) to Cd (mg kg^{-1}) ratios were 0:2000, 500:1500, 1000:1000, 1500:500 and 2000:0, respectively (Zhu et al. 2022). Briefly, the analytical grade Cd $(NO_3)_2$ and Na_3AsO_4 were dissolved with deionized water for the stock Cd (II) and As (V) solution, which was sprayed onto the dry soil evenly. The FBC was then added to the contaminated soil according to the mass ratio, and the dosages were calculated according to the results of the adsorption experiments. Furthermore, the mixes were placed in sealed containers under 25 °C, 60% humidity. After 7 days, the HMs leachability of the treated soil was tested.

2.3 Environmental experiments

In this section, the remediation effect and process of FBC were preliminarily explored in contaminated water and soils through batch adsorption tests and soil leaching toxic tests.

Table 2 The basic chemical and geotechnical properties of raw soil

Property	Value						
Main physical properties	pH	G_s	ω_p (%)	ω_L (%)	I_p	ω_o (%)	ρ_{dmax}
	7.38	2.68	17.60	34.29	16.69	17.93	1.80
Main chemical compositions (%)	SiO_2	Al_2O_3	Fe_2O_3	K_2O	CaO	MgO	Others
	66.34	16.92	8.17	2.85	2.04	1.53	2.15

G_s denotes specific gravity of raw soil; ω_p and ω_L denote atterberg limit; I_p denotes plastic index; ω_o denote optimal water content; ρ_{dmax} denotes maximum dry density (g cm^{-3}). The contents of other chemical compositions add up to 2.15%, and the relative content is less than 1%

2.3.1 Batch adsorption

The batch adsorption tests were conducted to evaluate the adsorption capacities of FBC for Cd (II) and As (V). Cd and As solutions of different concentrations were prepared with analytical grade $Cd(NO_3)_2$ and Na_3AsO_4. The initial pH of the mixture (7.0 ± 0.1) was coordinated by 0.1 mol L^{-1} NaOH or HCl. The FBC and HM solutions were mixed at a mass ratio of 1:1 in a polyethylene tube, which was oscillated at 120 revolutions per minute (rpm) to facilitate the reaction. The average value of three times was taken for each test results. The concentrations of As (V) and Cd (II) were measured by inductively coupled plasma (ICP Agilent 720ES) after reaction.

2.3.2 The leaching toxicity tests

The synthetic precipitation leaching procedure (SPLP) was applied to assess the toxicity of co-contaminated soils under the acid rain environment. For the SPLP test (US EPA Method 1312), the extraction was prepared by adding a 60/40 wt% sulfuric/nitric acid mixture and adjusting the pH to 4.20 ± 0.05. The concentration of As/Cd/Fe was determined by ICP Agilent 720ES.

2.4 Geotechnical tests

The topographic characteristics of As (V) and Cd (II) co-contaminated areas are mainly basins and hills. For the contaminated soil distributed on the slope, we focused on the geotechnical characteristics of aggregate distribution and soil shear strength.

2.4.1 Soil aggregate tests

The wet sieving test was conducted using Elliott's (1986) method. The mean weight diameter (MWD) is a parameter to measure the structural stability of soil aggregates (Bissonnais 1996). The MWD was calculated by Eq. (1):

$$MWD = \sum_{i=1}^{n} \overline{X_i} \times \overline{W_i} \quad (1)$$

where $\overline{X_i}$ is the mean diameter (mm), $\overline{W_i}$ is the percentage of aggregates, and n is the sieves' number.

2.4.2 Shear strength tests

A strain-controlled direct shear apparatus (ZJ Quadruplex) was used to measure the shear strengths of the contaminated soils. The cutting ring specimens (61.8 mm in internal diameter and 20 mm high) were made by isostatic pressing method within optimum moisture content. In each test, four vertical pressures were applied on the soil samples (100 kPa, 200 kPa, 300 kPa and 400 kPa) with 0.8 mm min^{-1} shear rate. The shear strength value was the stable value on shear stress–shear displacement curve, or if no stable value existed, it was the shear stress corresponding to the strain rate up to 20% (GB/T 50123–2019).

2.5 Analytic spectroscopic tests

Spectroscopic tests aim to reveal the phase transition during the stabilization process. Before testing, the contaminated soil samples were taken in the 0.075 mm powder phase. The crystalline phases of contaminated soils were analyzed by X-ray diffraction (XRD, Rigaku SmartLab SE) with 5° min^{-1} rate in the range of 10–80°. X-ray photoelectron spectroscopy (XPS, Thermo Scientific K-Alpha) was conducted to detect the elemental composition and chemical state of contaminated soils.

3 Results and discussion

3.1 Adsorption of FBC in solution

Figure 3 presents the adsorption isotherms for As (V) and Cd (II) by FBC. The calculated parameters of isothermal models are listed in Table 3. Math work found that the model parameters fitted better with the Langmuir model ($R^2 > 0.95$ for As, $R^2 > 0.97$ for Cd) than the Freundlich model ($R^2 > 0.92$ for As, $R^2 > 0.97$ for Cd), indicating that the adsorption process was a monolayer adsorption of As (V) and Cd (II). Based on Langmuir adsorption model, the maximum adsorption capacities of FBC for As (V) and Cd (II) were 31.96 and 129.31 mg g^{-1}, respectively. Compared to BC, the adsorption capacity of FBC for As increased by 34.19 times, while for Cd increased by 1.78 times. Therefore, the 97% removal of As was dependent on goethite NPs, while the another 3% removal was dependent on BC. Conversely, the 56% contribution of BC was stronger than the 44% contribution of goethite NPs for Cd removal.

The goethite NPs loaded on the FBC could obviously improve the adsorption capacities of BC for both Cd and As (Fig. 4). The immobilization of As is attributed to redox and complexation, while Cd is mainly dominated by electrostatic attraction and surface precipitation. For As (V) reaction on goethite, the goethite crystal must dissolve to facilitate Fe to build up binding sites (Wan et al. 2022). Part of AsO_4^{3-} could be hydrated to $HAsO_4^{2-}$ according to solution Eq. (2). Both AsO_4^{3-} and $HAsO_4^{2-}$ were adsorbed on FBC surface to from newly inner-sphere monodentate and bidentate complexes without obvious XRD peaks (Zhu et al. 2020b). The reaction of Cd^{2+} on the goethite surface can be described by the surface precipitation model (Bradl 2004). Parfitt

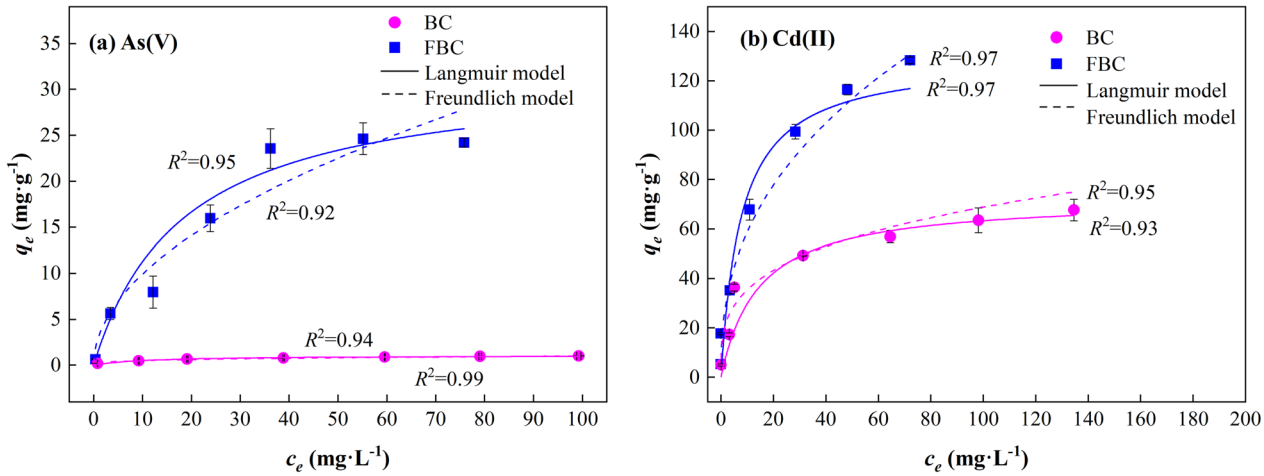

Fig. 3 Isotherm adsorption of As (V) and Cd (II) on FBC

Table 3 Langmuir and Freundlich parameters for the adsorption of As (V) and Cd (II) on BC and FBC

Adsorbent	Contaminant	Langmuir			Freundlich		
		k_L (L MG^{-1})	q_m (mg g^{-1})	R^2	K_F (mg$^{(1-n)}$ L^n g^{-1})	n	R^2
BC	As (V)	0.09 ± 0.02	1.07 ± 0. 48	0.94	0.25 ± 0.02	0.30 ± 0.02	0.99
	Cd (II)	0.11 ± 0.02	72.32 ± 2.86	0.93	18.20 ± 3.06	0.27 ± 0.04	0.95
FBC	As (V)	0.05 ± 0.01	31.96 ± 0.86	0.95	3.06 ± 1.25	0.51 ± 0.11	0.92
	Cd (II)	0.12 ± 0.02	129.31 ± 1.24	0.97	26.53 ± 3.86	0.38 ± 0.04	0.97

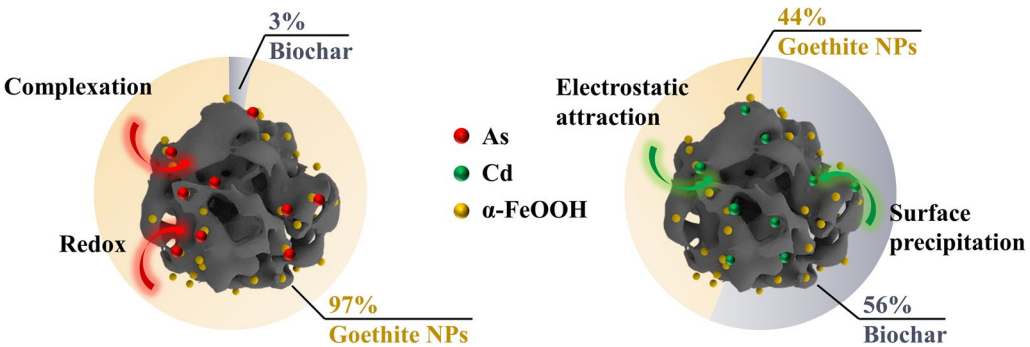

Fig. 4 The adsorption contributions of biochar and goethite NPs in FBC

(1976) classified the hydroxyl groups on the surface of goethite into *A*, *B*, and *C* classes. *A* class had higher activity by joining to one Fe^{3+} ion, while *B* and *C* classes had lower activity with two and three Fe^{3+}, respectively. At first Cd^{2+} formed surface complex on goethite Eq. (3a) and then Cd^{2+} precipitated as Cd $(OH)_2$ hydroxide on the surface (Eq. (3b)). The subsequent XRD test showed a new peak appearing at 30.52° belonging to Cd $(OH)_2$ (PDF# 71–2137) in Sect. 3.4, supporting the above hypothesis on the Cd precipitate with hydroxyl group on the goethite surface.

$$AsO_4^{3-} + H_2O \rightarrow HAsO_4^{2-} + OH^- \quad (2a)$$

$$S-FeOH + AsO_4^{3-} + H_2O \rightarrow S-FeAsO_4^{2-} + OH^- \quad (2b)$$

$$S-FeOH + HAsO_4^{2-} + H_2O \rightarrow S-FeH_2AsO_4 + 2OH^- \quad (2c)$$

$$S-OH+Cd^{2+}+H_2O \leftrightarrow S-O-CdOH_2^{+}+H^{+} \quad (3a)$$

$$S-O-CdOH_2^{+}+Cd^{2+}+SH_2O \leftrightarrow\equiv S-O-CdOH_2^{+}+Cd(OH)_2\downarrow+2H^{+} \quad (3b)$$

Furthermore, the influence of HMs initial concentration on the FBC removal rate is presented in Additional file 1: Fig. S1. With an increasing As concentration from 1 to 100 mg L^{-1}, the removal rate dropped from 64% to 24.19%. It can be explained by the fact that PO_4^{3-}can diffuse into the meso- and micro-pores of goethite, reducing specific surface area (Faria et al. 2014). Given the similarity of AsO_4^{3-} and PO_4^{3-}, it seems reasonable to speculate that AsO_4^{3-} may block pores on goethite and hinder the diffusion. As a result, their adsorption capacities are affected. In Additional file 1: Fig. S1b, the adsorption quantity of Cd by FBC grew from 5.00 to 128.29 mg g^{-1} with the increase of initial concentration from 5 to 200 mg L^{-1}. However, the removal rate maintained at 100% till 20 mg L^{-1}, then gradually decreased and reached 64.02% at 200 mg L^{-1}. The FBC provided a fixed number of hydroxyl active sites for Cd adsorption, similar to the pattern for most adsorbent (Fan et al. 2020). The more cadmium ions, the fewer corresponding adsorption sites.

3.2 Leaching characteristics of treated co-contaminated soils

In untreated samples (Fig. 5), the As leaching concentration gradually increased with the increase of As content in co-contaminated soils from As: Cd = 0: 2000 to 2000: 0 (0, 4.72, 21.73, 43.67, 74.50 mg L^{-1}), implying that AsO_4^{3-} had sufficiently reacted with the soil. The soil particles have a fixing effect on As (0, 81.11%, 56.54%, 41.77% and 25.50%), which was gradually weakened with the As content rising. On this basis, incorporation of 2% FBC reduced by 25.31% on average of the As leaching concentration (0, 3.31, 17.13, 28.20, 63.50 mg L^{-1}). When the FBC content increased to 6%, the As leaching concentration was decreased by 79.30% as a whole (0, 0, 2.43, 9.21, 31.83 mg L^{-1}), not entirely disappeared yet. As leaching concentration was less than 0.02 mg L^{-1} until the dosage of FBC was increased to 10%, meeting the regulation limit of China's ground/surface water (GB/T 14848-2017; GB 3838-2002). Cd leaching concentrations of untreated contaminated soils were 81.88, 56.66, 29.69, 11.08, 0 mg L^{-1}, proving that the mobility of Cd was greater than As under the same action time while the fixing effect of soil particles was poor (18.12%, 24.45%, 40.62%, 55.68% and 0). When 2% FBC was added, the Cd leaching concentration could be completely controlled below 1 mg L^{-1}, which indicated that the 2% FBC-treated contaminated soil might not pose the risk to the surrounding water/soil under acid rain erosion. For co-contaminated soil with As: Cd = 1000: 1000, the leaching concentrations of As (V) and Cd (II) were 21.73 and 29.69 mg L^{-1} in untreated soils, 17.13 and 0.02 mg L^{-1} in 2% FBC-treated soils, 2.43 and 0 mg L^{-1} in 6% FBC-treated soils, while 0.02 and 0 mg L^{-1} in 10% FBC-treated soils. In addition, the leaching concentration of iron (Fe) in soil was below 0.02 mg L^{-1}, indicating that iron on FBC would not escape into soil to avoid extra environmental burden.

The theoretical demands of FBC for stabilization of co-contaminated soils should be the FBC requirement for As (V) and Cd (II) immobilization. According to the calculated amount of FBC for As (V) and Cd (II) in solution from Sect. 3.1, the theoretical needed demands of FBC for stabilizing 2000 mg kg^{-1} single Cd or As contaminated soils should be 1.5% and 6%, while the actual dosages were 2% and 10%, respectively. The actual dosages were greater than the theoretical demands because FBC contacted with HMs ions as well as soil particles at the same time. The interface between goethite and kaolin was cemented by the formation of hydrogen bond, which consumed strong adsorption sites binding to HMs (Parfitt 1989). Consequently, part of the highly active potentials

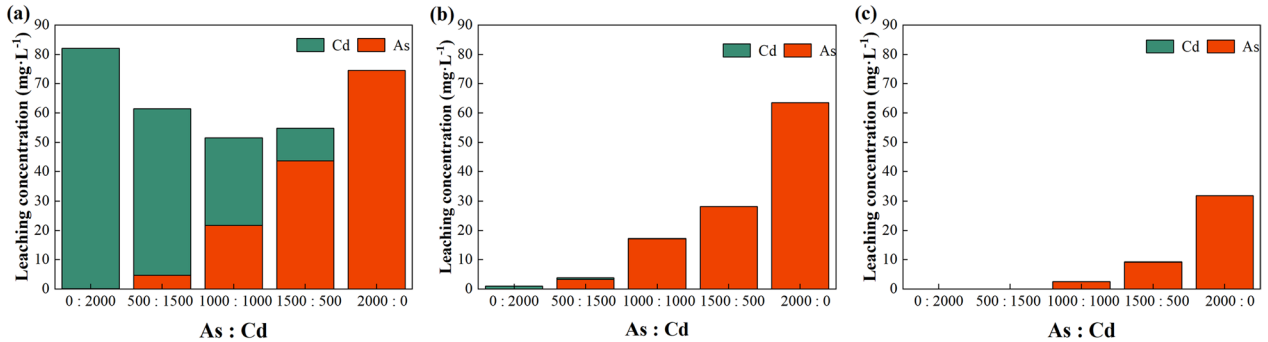

Fig. 5 SPLP leaching concentrations of As and Cd with different FBC dosages in co-contaminated soils: **a** no FBC, **b** 2% FBC dosage, and **c** 6% FBC dosage

reacted with clay minerals, leading to the actual dosages required for stabilization generally being on average 57% higher than the theoretical values. Moreover, in co-contaminated soils of As (V) and Cd (II), the actual dosages of FBC were not the simple addition of the As demands and the Cd demands, but a cross relationship determined by the concentrations of contaminants. The formula for calculating the actual dosages (D_{ac}) of FBC is as follows Eq. (4). When the As concentration exceeds 4 times that of Cd, the actual dosages of FBC depend on the As demands, and vice versa on the demands of Cd.

$$D_{ac} = \max[D_{ac}(\mathrm{As}), D_{ac}(\mathrm{Cd})] = \begin{cases} D_{ac}(\mathrm{As}), c_{As} \geq 4c_{Cd} \\ D_{ac}(\mathrm{Cd}), c_{As} < 4c_{Cd} \end{cases} \quad (4)$$

where D_{ac} is the actual dosages of FBC, D_{ac}(As) and D_{ac}(Cd) are the FBC demands of As (V) and Cd (II), respectively,c_{As} and c_{Cd} are the concentrations of As (V) and Cd (II) in soils, respectively.

3.3 Geotechnical properties of treated co-contaminated soils

3.3.1 Soil aggregate distribution

Grades of aggregates include small macroaggregates (1–2 mm and 0.25–1 mm), microaggregates (0.053–0.25 mm), and mineral fraction (0–0.053 mm) (Elliott 1986). As showed in Fig. 6, small macroaggregates of raw soil increased by 27% after addition of 10% FBC, which was consistent with the prior research results (Sun and Lu 2014). The untreated single Cd contaminated soil (As:Cd = 0:2000) had the most aggregates in the range of 1–2 mm, while the untreated single As contaminated soil (As:Cd = 2000:0) had the most soil particles of microaggregates and mineral fraction. Simultaneously, the higher As content, the worse stability of the soil aggregates with smaller MWD. Both As (V) and Cd (II) can redistribute soil aggregates by changing charge potential, and bound water film of soil particle surface. The Cd^{2+} contributed soil particles to soil aggregates, while AsO_4^{3-} dispersed aggregates in clayey soils (Elliott 1986; Du et al. 2014). After 10% of FBC addition, 0.25–1 mm and 0.053–0.25 mm aggregates were the major fractions present, with the small macroaggregates (0.25–1 mm) growing by 18.8% and microaggregates reducing by 16.4%. The MWD was enhanced by about 0.15 mm as a whole and nearly remained the same level with different concentration ratios of As (V) and Cd (II) in the contaminated soils (Table 4). Additionally, the content of mineral fraction increased with As concentration and caught the maximum in As: Cd = 2000: 0.

Table 4 The MWD (mm) of As (V) and Cd (II) co-contaminated soils

Soil sample	Untreated co-contaminated soil	Co-contaminated soils stabilized by FBC
Raw soil	0.46	0.62
0:2000	0.48	0.61
500:1500	0.4	0.53
1000:1000	0.4	0.51
1500:500	0.38	0.51
2000:0	0.33	0.49

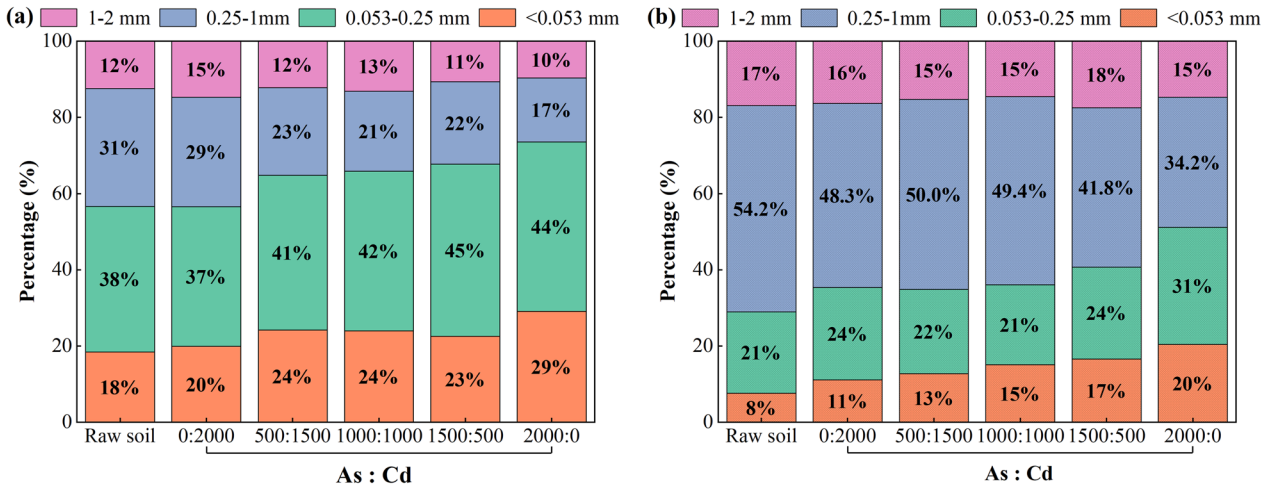

Fig. 6 Soil aggregates of As (V) and Cd (II) co-contaminated soils: **a** untreated co-contaminated soils and **b** co-contaminated soils stabilized by FBC

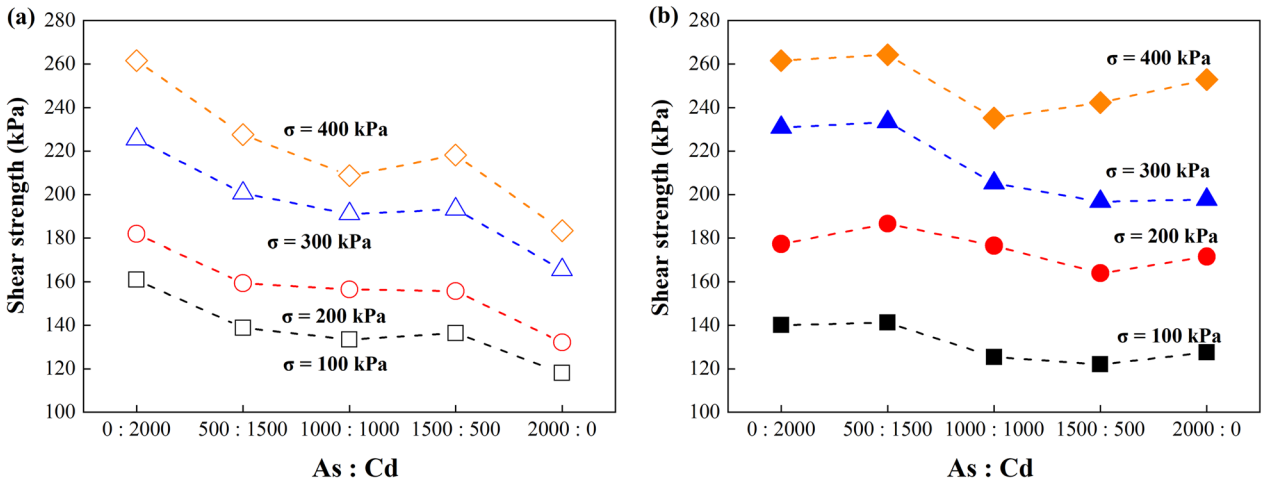

Fig. 7 Shear strength of As (V) and Cd (II) co-contaminated soils: **a** untreated co-contaminated soils and **b** co-contaminated soils stabilized by FBC

Table 5 The cohesion and internal friction angle of As (V) and Cd (II) co-contaminated soils

As: Cd	Untreated co-contaminated soil		Co-contaminated soil stabilized by FBC	
	c (kPa)	φ (°)	c (kPa)	φ (°)
0:2000	121.10	19.29	97.81	22.78
500:1500	104.76	17.22	102.35	22.78
1000:1000	105.21	14.57	96.1	19.80
1500:500	107.30	15.64	82.8	21.30
2000:0	92.38	12.95	86.8	21.80

3.3.2 Direct shear strengths

The shear strengths for different co-contaminated soils before and after treatment with FBC are shown in Fig. 7. The shear strengths of co-contaminated soils stabilized by FBC with different As (V) and Cd (II) ratios were found to be closer compared to untreated co-contaminated soils, with the difference controlled to 8.77–33.1 kPa instead of 42.98–78.32 kPa. This revealed that FBC weakened the effect of HMs on soil properties. In particular, the shear strength of stabilized soil As:Cd = 0:2000 slightly decreased by 3.29%, whereas increased by 8.34% on the average in the soil samples containing As (the other four soils). As discussed later in Sect. 4.2. FBC is beneficial for increasing the shear strength of the contaminated soils with anions. Nevertheless, the change in shear strength for contaminated soils containing cations depends on the extent to which the substitution of cations by FBC affects the soil particle aggregation. The calculated shear strength parameters of the contaminated soils are shown in Table 5. The cohesions of stabilized soil decreased but the internal friction angles grew. The intervention of FBC blocked the damage of HMs to the soil and balanced the charge system in soils, which reduced the electrostatic attraction between particles and led to the decrease of cohesions. At the same time, the internal friction angles increased because the aggregate distribution of soil particles was changed to be larger, making the occlusal friction stronger. Furthermore, as a small particle, the uneven surface of FBC expanded the sliding friction.

3.4 Phase transition and microstructure in stabilization process

The XRD patterns and XPS spectra of the FBC stabilized As (V) and Cd (II) co-contaminated soils are shown in Fig. 8. After stabilization, newly formed mineral crystals were found in the XRD pattern, including angelellite (Fe_4O_3 $(AsO_4)_2$, PDF# 83–1554), cadmium hydroxide ($Cd(OH)_2$, PDF# 71-2137) and cadmium arsenate ($Cd_3(AsO_4)_2$, PDF# 71-2080) as shown in Fig. 8a. These minerals could effectively bind the aggregates, increase the surface roughness and internal friction between the soil particles, thereby enhancing the shear strength. The full spectrums of the samples display the main core level peak for C 1 s, Fe 2p, Cd 3d, and As 3d. High-precision narrow region spectra of As 3d, Cd 3d, Fe 2p, and O 1 s were collected to further explore the chemical states and reaction mechanisms. The deconvolution results of As 3d fine-spectrum indicated that As was divided into two chemical states, As (V) at 44.9 eV and As (III) at 45.7 eV (Ma et al. 2022). Despite the initial As (V) was partially reduced to As (III) caused by the redox of surface Fe (II) (Perez et al. 2019), the immobilized As was stably bound to FBC and clay minerals during the

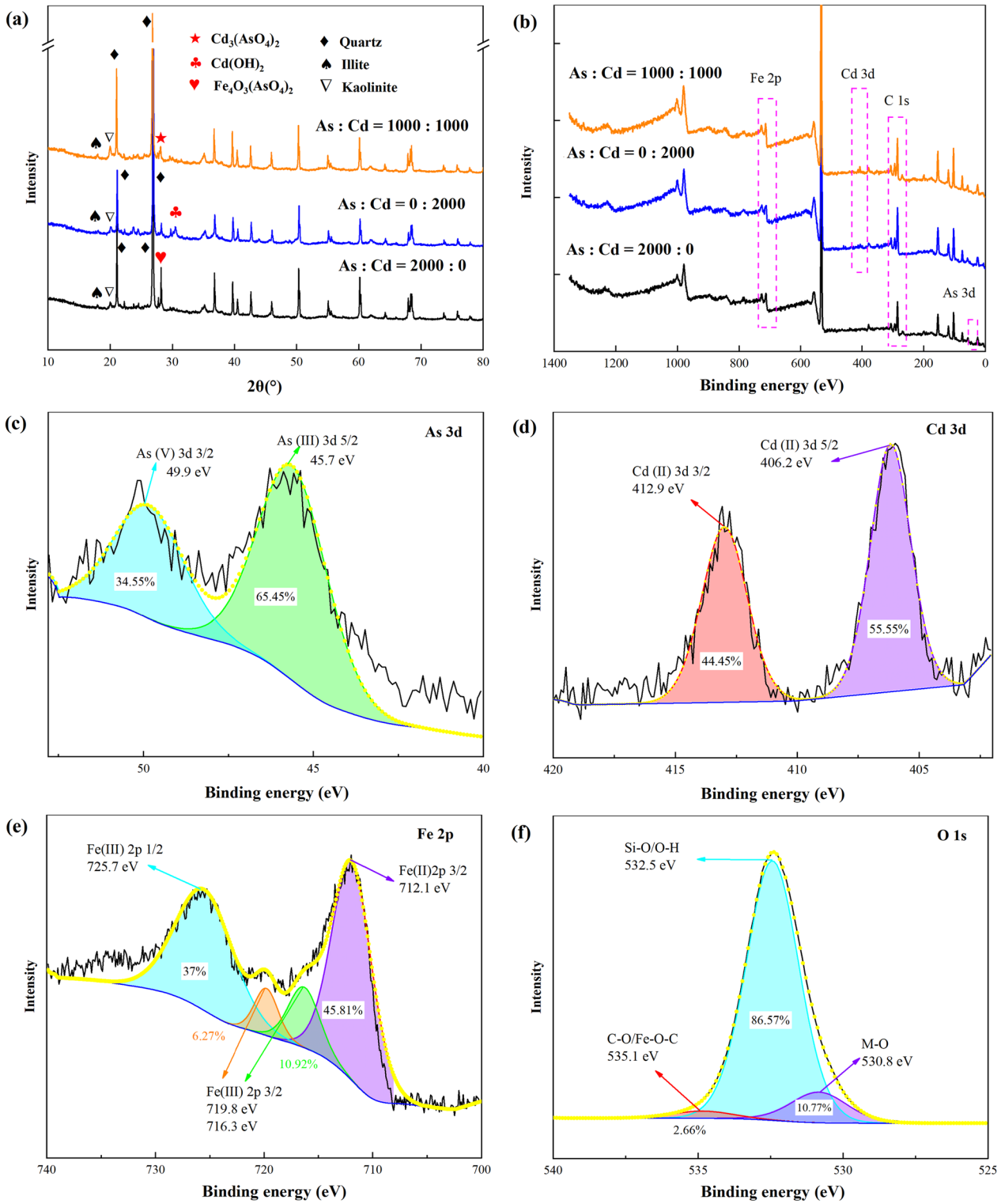

Fig. 8 Spectroscopic of As (V) and Cd (II) co-contaminated soils stabilized by FBC: **a** XRD pattern, **b** XPS full spectrum, and **c–f** high-precision narrow region spectra of As 3d, Cd 3d, Fe 2p, and O 1s

stabilization reaction. Therefore, the stabilization effect would not be compromised because As was prevented from being released into the environment from start to finish. Besides, the XPS spectra of Cd 3d consisted of the peak at 406.2 eV and 412.9 eV, associated with Cd 3d5/2 (Cd–Fe hydroxide or Cd–As) and Cd 3d3/2 (Cd $(OH)_2$) (Zhu et al. 2022). Two main components of Fe 2p were considered to be 54.19% Fe (III) and 45.81% Fe (II). The O 1s XPS spectra were deconvoluted into C–O/Fe–O–C, Si–O/O–H, and M–O, respectively. The M–O peak of 10.77% may be due to the Al–O or Cd–O/As–O. Meanwhile, the Fe–O–C/C–O content was 2.66%, mainly attributed to the formation of Cd/As–Fe inner-sphere complex (Fan and Zhang 2018). To sum up, the changes in chemical form and crystalline phase of HMs occur during the stabilization process caused by chemical precipitation, redox and complexation reactions.

3.5 Stabilization mechanisms of FBC to HMs contamination in soils

Comparison of the HMs adsorption of FBC in solution and soils revealed that the actual dosages required for stabilization for co-contaminated soils was generally 57% higher on average than the theoretical values in solution, indicating that FBC in soil was not target binding with HMs. Some FBC interacted directly with soil particles. According to the analysis of soil aggregate change in the raw soil and treated raw soil, FBC promoted the soil macroaggregates (1–2 mm and 0.25–1 mm) by 27%, but reduced the microaggregates (0.053–0.25 mm) by 16.6%, and mineral fraction (0–0.053 mm) by 10.4%. It may be caused by electrostatic attraction between soil particles and FBC as well as hydrogen bonding of the hydroxyl group on the surface of FBC. Among the untreated soils, the Cd contaminated soil (As:Cd = 0:2000) had the largest amount of small macroaggregates (1–2 mm and 0.25–1 mm), which was related to the fact that Cd^{2+} could compress the diffusion double layer (DDL) thickness of clay particles, making it easier to agglomerate into larger soil aggregations (Spielman and Friedlander 1974). After stabilization by FBC, the agglomeration effect of Cd^{2+} on the soil particles was destroyed. As a result, the aggregate change (1–2 mm) of the treated Cd contaminated soil was the smallest (1%), and the shear strength decreased slightly by 3.29%. In contrast, the AsO_4^{3-} can thicken the DDL of clay particles, dispersing soil particles to small aggregates with relative flocculation structure, which reduces the friction coefficient between soil particles and the shear strengths (Foad and Haddad 2015). As a consequence, the mineral fraction (0–0.053 mm) of As contaminated soil (As:Cd = 2000:0) was the most in the untreated soils. The contents of largest particles

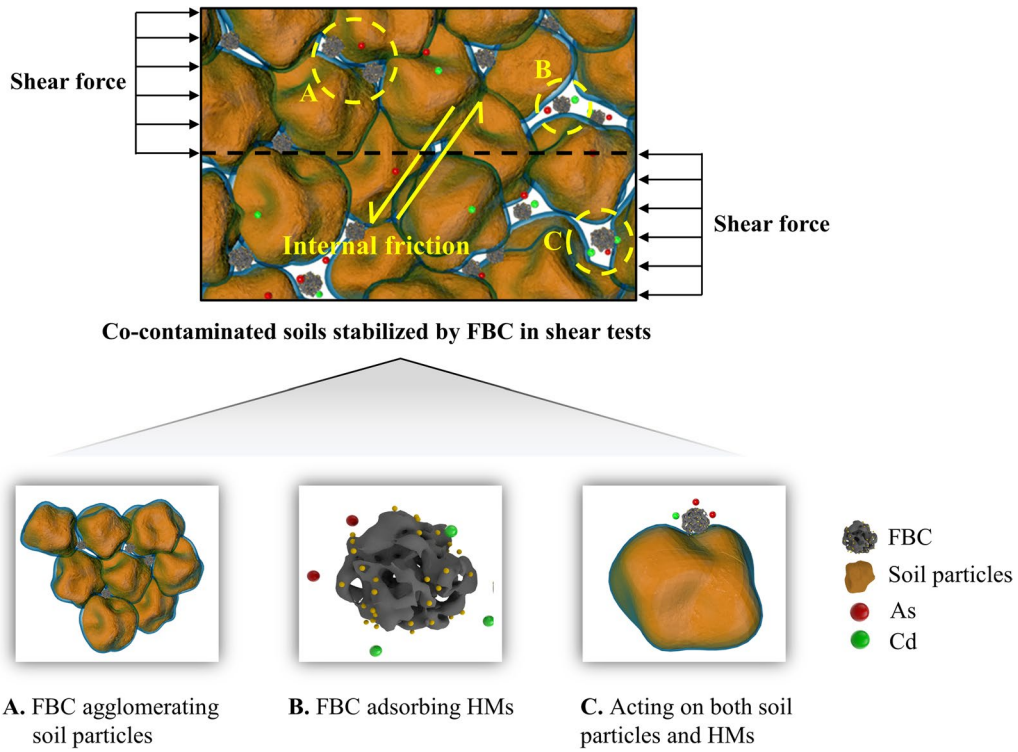

Fig. 9 Three modes of FBC in the co-contaminated soils

(1–2 mm) in the four soil samples containing As (the other four soils) increased by about 4.25% after stabilization, enhancing the force between adjacent particles and leading to the shear strength increase by 8.34% on average.

The intervention of FBC prevented the damage of HMs to the soils. The effects of FBC added into the contaminated soils comprised three modes (Fig. 9): (*A*) FBC combining soil particles, (*B*) FBC adsorbing HMs, and (*C*) FBC acting on both soil particles and HMs. Mode *A* served as the central nucleation site for the agglomeration of soil particles through the pore effect of biochar and the hydrogen bonding of goethite NPs on the surface, which improved aggregate stability and soil cohesion. Mode *B* prevented the damage of HMs ions on soil particles through physical adsorption, chemical complexation and precipitation. However, since the surface charge of FBC was equilibrated after adsorption, this mode of FBC existed in the form of electrically neutral small particles to fill the pores. In mode *C,* FBC was attached to soil particles, which enhanced the friction between the adjacent aggregates due to the rough and porous microstructure of BC surface. Also, this part was the most unstable when suffering external forces or environmental erosion. In summary, the FBC can effectively stabilize As (V) and Cd (II) co-contaminated soils through two ways: one is that FBC immobilizes the As (V) and Cd (II) to reduce the toxicity of soils, including electrostatic attraction, precipitation, complexation and redox, thus achieving stabilization effect; and another is that newly formed crystal minerals and FBC bind aggregates and increase the surface roughness of soil particles, thereby improving the strength of soil.

3.6 Evaluation of soil reutilization

Soil reutilization quality can be described in terms of environmental safety and geotechnical reliability. The leaching toxicity of HMs can be applied to characterize environmental safety of soil. The indexes of geotechnical reliability included the cohesion, internal friction angle, and the MWD of aggregates. In this section, the TOPSIS method (Hwang and Yoon 1981; Li et al. 2022) was employed to evaluate the relative advantages of soil reutilization based on four sub-indices. The detailed calculation steps are shown in Additional file 1 with relevant calculation data shown in Additional file 1: Table S1. The index values of various soil samples are calculated by:

$$S_i = \frac{D_i^-}{D_i^+ + D_i^-} \tag{5}$$

where S_i is index value between zero and one. Soil reutilization quality increases as S_i approaches 1. D_i^+ and D_i^- are the distance to the positive/negative ideal solution from row vector (**i**) to the ideal solution.

The evaluation results are shown in Additional file 1: Fig. S2. Soil reutilization quality increased significantly after stabilization of FBC. The index values of co-contaminated soils stabilized by FBC were between 0.76 and 0.83 with a "Satisfactory" or "Good" level, even better than raw soil with a value of 0.62. In contrast, the index values of untreated co-contaminated soils were between 0.16 and 0.46 with a "Poor" or "Fair" level, with the lowest 0.16 in As: Cd = 1000:1000, showing that the co-contamination caused more severe geo-environmental problems. Furthermore, the change trends of four sub-indices are shown in Fig. 10. For untreated contaminated soils, the reduction of environmental safety was the main reason for the decline of soil reutilization quality. However, FBC stabilized contaminated soils had higher environmental safety, MWD of aggregates and internal friction angle, resulting in the increasing of soil reutilization quality.

4 Conclusions

The main conclusions are drawn as follows:

1. The FBC could immobilize As (V) and Cd (II) in both polluted water and contaminated soils. The dosages of FBC required in contaminated soils generally are about 57% higher than those in polluted water. When the concentration of As exceeds 4 times that of Cd, the dosage of FBC is determined by the concentration of As; otherwise, it is determined by the concentration of Cd.
2. After stabilization by FBC, soil aggregates transformed from mineral fraction (0–0.053 mm) and microaggregates (0.053–0.25 mm) to small macroaggregates (0.25–2 mm). The shear strength of stabilized soils containing As is increasing, while the opposite is true for soils contaminated by single Cd.
3. The stabilization mechanisms include: (1) HMs immobilization. FBC immobilizes the As (V) and Cd (II) to reduce the soil toxicity by electrostatic attraction, precipitation, complexation and redox; and (2) soil agglomeration. Newly formed crystal minerals and soil particles bound with FBC increase the friction of adjacent aggregates, thereby improving the shear strength of soils.
4. The soil reutilization was evaluated through TOPSIS method, where four geo-environmental factors, including cohesion, internal friction angle, mean weight diameter, and leaching toxicity of HMs are

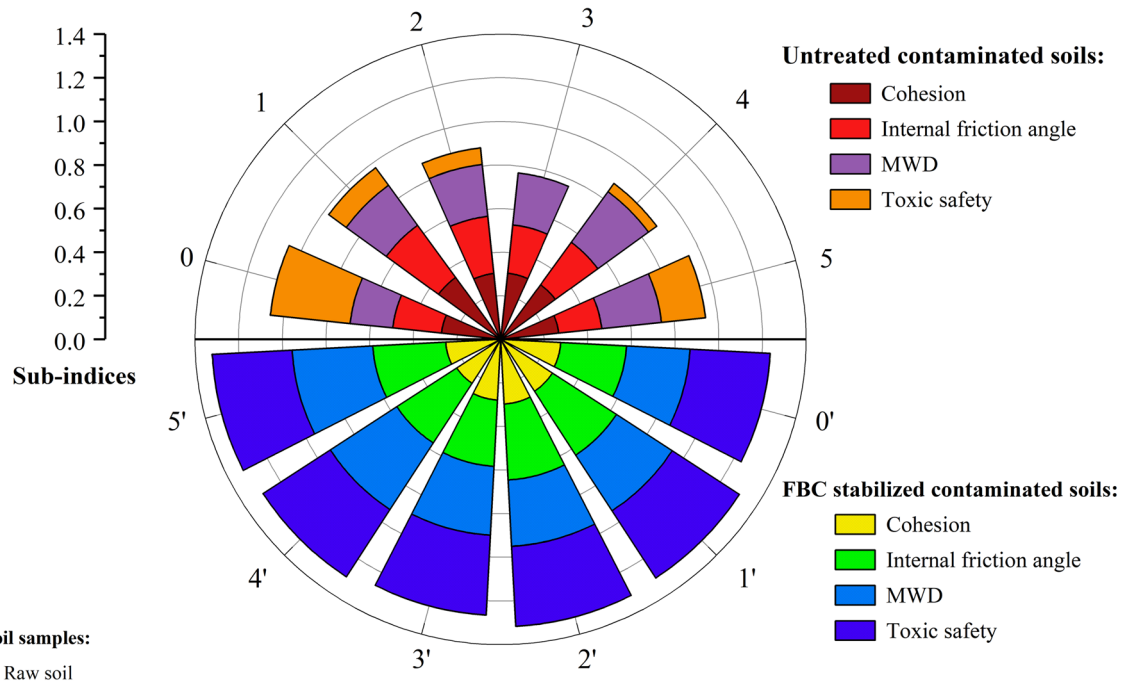

Fig. 10 Trends of four sub-indices in TOPSIS evaluation method

incorporated. Soil reutilization quality increased significantly after stabilization by FBC, from 0.16 to 0.46 with a "Poor" or "Fair" level to 0.76–0.83 with a "Satisfactory" or "Good" level.

The study findings confirm the potential of reusing agricultural wastes in the field of HMs-contaminated soil stabilization, so as to achieve the purpose of treating the wastes with wastes and carbon sequestration. However, there are still some limitations about this research, including: (1) The experimental time conducted was relatively short, and long-term effects were not taken into account. Additionally, the stabilization of heavy metal contaminated sites is necessary to perform to explore FBC's engineering applicability; (2) The actual engineering often suffers from complex environmental effects (e.g., drying–wetting and freezing–thawing cycles), and the impact of these factors on the deterioration of FBC' stabilization effectiveness is unknown; (3) The co-contaminated sites often exist multiple HMs, including zinc (Zn), copper (Cu), nickel (Ni), etc., and it is crucial to explore the coupling stability mechanism of FBC on them. Generally, the contamination situation and remediation standard of the site need to be comprehensively considered before stabilizing with FBC.

Supplementary Information

The online version contains supplementary material available at https://doi.org/10.1007/s42773-023-00253-7.

Additional file 1: Table S1. The raw testing date and calculation results. **Figure S1.** Effect of initial concentration on the removal of heavy metals by FBC: (a) As and (b) Cd. **Figure S2.** TOPSIS evaluation results and its corresponding soil reutilization levels.

Acknowledgements
The authors appreciate the financial support from the National Key Research and Development Program, China (Grant No. 2019YFC1804002), the National Natural Science Foundation of China (Grant No.42177163) and the CAS Pioneer Hundred Talents Program in China.

Author contributions
All authors contributed to the study conception and design. Material preparation, data collection and analysis were performed by CF, JL, WJ, JL and QX. The first draft of the manuscript was written by CF and all authors commented on previous versions of the manuscript. All authors read and approved the final manuscript.

Funding
This work was supported by the National Key Research and Development Program, China (Grant No. 2019YFC1804002), the National Natural Science Foundation of China (Grant No.42177163) and the CAS Pioneer Hundred Talents Program in China.

Availability of data and materials
The datasets used or analyzed during the current study are available from the corresponding author on reasonable request.

Declarations

Competing interests

The authors have no relevant financial or non-financial interests to disclose.

Author details

[1]State Key Laboratory of Geomechanics and Geotechnical Engineering, Institute of Rock and Soil Mechanics, Chinese Academy of Sciences, Wuhan 430071, China. [2]University of Chinese Academy of Sciences, Beijing 100049, China. [3]Hubei Province Key Laboratory of Contaminated Sludge and Soil Science and Engineering, Wuhan 430071, China. [4]IRSM-CAS/HK PolyU Joint Laboratory on Solid Waste Science, Wuhan 430071, China.

Received: 27 November 2022 Revised: 4 August 2023 Accepted: 11 August 2023
Published online: 04 September 2023

References

Abdelrhman F, Gao JY, Ail G, Wan N, Sharaf A, Hu HQ (2022) Assessment of goethite modified biochar on the immobilization of cadmium and arsenic and uptake by Chinese cabbage in paddy soil. Arch Agron Soil Sci 69:1039–1054. https://doi.org/10.1080/03650340.2022.2050370

Bissonnais YL (1996) Aggregate stability and assessment of soil crustability and erodibility: I. Theory and methodology. Eur J Soil Sci 47:425–437. https://doi.org/10.1111/j.1365-2389.1996.tb01843.x

Bradl HB (2004) Adsorption of heavy metal ions on soils and soils constituents. J Colloid Interface Sci 277:1–18. https://doi.org/10.1016/j.jcis.2004.04.005

Du YJ, Jiang NJ, Li SY, Jin F, Singh DN, Puppala AJ (2014) Engineering properties and microstructural characteristics of cement-stabilized zinc-contaminated kaolin. Can Geotech J 51:289–302. https://doi.org/10.1139/CGJ-2013-0177

Elliott ET (1986) Aggregate structure and carbon, nitrogen, and phosphorus in native and cultivated soils. Soil Sci Soc Am J 50:627–633. https://doi.org/10.2136/sssaj1986.03615995005000030017x

Fan CH, Zhang YC (2018) Environmentally friendly remediation of lead/cadmium co-contaminated loess soil in northwestern China using a humificated straw solution. Environ Sci Pollut Res 25:25243–25254. https://doi.org/10.1007/s11356-018-2601-2

Fan JJ, Cai C, Chi HF, Reid BJ, Coulon F, Zhang YC, Hou YW (2020) Remediation of cadmium and lead polluted soil using thiol-modified biochar. J Hazard Mater 388:122037. https://doi.org/10.1016/j.jhazmat.2020.122037

Faria MCS, Rosemberg RS, Bomfeti CA, Monteiro DS, Barbosa F, Oliveira LCA, Rodriguez M, Pereira MC, Rodrigues JL (2014) Arsenic removal from contaminated water by ultrafine δ-FeOOH adsorbents. Chem Eng J 237:47–54. https://doi.org/10.1016/j.cej.2013.10.006

Foad C, Haddad A (2015) Strength properties of soft clay treated with mixture of nano-SiO2 and recycled polyester fiber. J Rock Mech Geotech Eng 7:367–378. https://doi.org/10.1016/j.jrmge.2015.03.013

Ganesan SP, Bordoloi S, Ni J, Sizmur T, Garg A, Sekharan S (2020) Exploring implication of variation in biochar production on geotechnical properties of soil. Biomass Convers Bior. https://doi.org/10.1007/s13399-020-00847-2

GB 3838-2002 (2002) Environmental quality standards for surface water. Beijing: State Environmental Protection Administration of China, General Administration of Quality Supervision, Inspection and Quarantine of the People's Republic of China.

GB/T 14848-2017 (2017) Standard for groundwater quality. Beijing: General Administration of Quality Supervision, Inspection and Quarantine of the People's Republic of China, China National Standardization Administration.

GB/T 50123-2019 (2019) Standard for soil test method. Beijing: Ministry of Housing and Urban-Rural Development of the People's Republic of China, China National Standardization Administration.

Hwang CL, Yoon K (1981) Multiple attribute decision making: methods and applications. Springer-Verlag, New York

Irshad MK, Noma NA, Wang Y, Yin YJ, Chen C, Shang JY (2022) Goethite modified biochar simultaneously mitigates the arsenic and cadmium accumulation in paddy rice (Oryza sativa) L. Environ Res 206:112238. https://doi.org/10.1016/j.envres.2021.112238

Li Y, Wei ML, Yu BW, Liu L, Xue Q (2022) Thermal desorption optimization for the remediation of hydrocarbon-contaminated soils by a self-built sustainability evaluation tool. J Hazard Mater 436:129156. https://doi.org/10.1016/j.jhazmat.2022.129156

Li YB, Zhang MM, Xu R, Lin HZ, Sun XX, Xu FQ, Gao P, Kong TL, Xiao EZ, Yang N, Sun WM (2021) Arsenic and antimony co-contamination influences on soil microbial community composition and functions: relevance to arsenic resistance and carbon, nitrogen, and sulfur cycling. Environ Int 153:106522. https://doi.org/10.1016/j.envint.2021.106522

Lin LY, Li JC, Yang X, Yan XL, Feng TT, Liu ZS, Deng YR, Zhou HY (2020) Simultaneous immobilization of arsenic and cadmium in paddy soil by Fe-Mn binary oxide: a field-scale study. Elementa Sci Anthrop 8:094. https://doi.org/10.1525/elementa.2020.094

Ma ZH, Li JS, Xue Q, Zhan BJ, Chen X, Wan Y, Zhao YQ, Sun YH, Poon CS (2022) Deep insight on mechanism and contribution of As (V) removal by thermal modification waste concrete powder. Sci Total Environ 807:150764. https://doi.org/10.1016/j.scitotenv.2021.150764

Mohammad EH, Vaezi I, Mahboubi AA (2020) Evaluation of solidification/stabilization in arsenic-contaminated soils using lime dust and cement kiln dust. B Eng Geol Environ 79:1683–1692. https://doi.org/10.1007/s10064-019-01698-6

Parfitt RL (1989) Phosphate reactions with natural allophane, ferrihydrite and goethite. J Soil Sci 40:359–369. https://doi.org/10.1111/j.1365-2389.1989.tb01280.x

Perez JPH, Tobler DJ, Thomas AN, Freeman HM, Dideriksen K, Radnik J, Benning LG (2019) Adsorption and reduction of arsenate during the Fe2+-induced transformation of ferrihydrite. ACS Earth Space Chem 6:884–894. https://doi.org/10.1021/acsearthspacechem.9b00031

Schwertmann U, Cornell RM (2000) Iron oxides in the laboratory: preparation and characterization. Wiley-VCH, Weinheim

Spielman LA, Friedlander SK (1974) Role of the electrical double layer in particle deposition by convective diffusion. J Colloid Interface Sci 46:22–31. https://doi.org/10.1016/0021-9797(74)90021-6

Sun FF, Lu SG (2014) Biochars improve aggregate stability, water retention, and pore-space properties of clayey soil. J Plant Nutr Soil Sci 177:26–33. https://doi.org/10.1002/jpln.201200639

Takeno N (2005) Atlas of Eh-pH diagrams. Geological Survey of Japan Open File Report No.419. National Institute of Advanced Industrial Science and Technology Research Center for Deep Geological Environments, Tsukuba, Japan.

US Epa (2003) Method 1312: synthetic precipitation leaching procedure. US EPA, Washington DC

Vinh ND, Thao PTP, Hanh NT (2019) Feasibility of goethite nanoparticles for Pb (II) and Cd (II) removal from aqueous solution. Vietnam J Chem 57:281–287. https://doi.org/10.1002/vjch.201960027

Vithanage M, Herath I, Joseph S, Bundschuh J, Bolan N, Ok YS, Kirkham MB, Rinklebe J (2017) Interaction of arsenic with biochar in soil and water: a critical review. Carbon 113:219–230. https://doi.org/10.1016/j.carbon.2016.11.032

Wan SL, Li Y, Cheng S, Wu GW, Yang X, Wang Y, Gao LM (2022) Cadmium removal by FeOOH nanoparticles accommodated in biochar: Effect of the negatively charged functional groups in host. J Hazard Mater 421:126807. https://doi.org/10.1016/j.jhazmat.2021.126807

Wang ZP, Shen R, Ji SB, Xie LK, Zhang HB (2021) Effects of biochar derived from sewage sludge and sewage sludge/cotton stalks on the immobilization and phytoavailability of Pb, Cu, and Zn in sandy loam soil. J Hazard Mater 419:126468. https://doi.org/10.1016/j.jhazmat.2021.126468

Wang XB, Ma S, Wang XL, Cheng T, Dong JN, Feng K (2022) The mechanism of Cu^{2+} sorption by rice straw biochar and its sorption-desorption capacity to Cu^{2+} in soil. B Environ Contam Tox 109:562–570. https://doi.org/10.1007/s00128-022-03538-y

Xu C, Xiang Q, Zhu HH, Wang S, Zhu QH, Huang DY, Zhang YZ (2018) Effect of biochar from peanut shell on speciation and availability of lead and zinc in an acidic paddy soil. Ecotoxicol Environ Saf 164:554–561. https://doi.org/10.1016/j.ecoenv.2018.08.057

Xue Q, Zhang LT, Hu LM, Du YJ (2020) Environmental geotechnics: state-of-the-art of theory, testing and application to practice. China Civil Eng J 53:80–94. https://doi.org/10.15951/j.tmgcxb.2020.03.010

Yang QQ, Li ZY, Lu XN, Duan QN, Huang L, Bi J (2018) A review of soil heavy metal pollution from industrial and agricultural regions in China:

pollution and risk assessment. Sci Total Environ 642:690–700. https://doi.org/10.1016/j.scitotenv.2018.06.068
Zhang YP, Gu K, Tang CS, Shen ZT, Narala GR, Shi B (2020) Effects of biochar on the compression and swelling characteristics of clayey soils. Int J Geosynth Ground Eng 6:22. https://doi.org/10.1007/s40891-020-00206-1
Zhou PF, Adeel M, Guo M, Ge L, Shakoor N, Li MS, Li YB, Wang GY, Rui YK (2022) Characterisation of biochar produced from two types of chestnut shells for use in remediation of cadmium-and lead-contaminated soil. Crop Pasture Sci 74:21297. https://doi.org/10.1071/CP21297
Zhu SH, Qu T, Irshad MK, Shang JY (2020a) Simultaneous removal of Cd (II) and As (III) from co-contaminated aqueous solution by α-FeOOH modified biochar. Biochar 21:81–92. https://doi.org/10.1007/s42773-020-00040-8
Zhu SH, Zhao JJ, Zhao N, Yang X, Chen C, Shang JY (2020b) Goethite modified biochar as a multifunctional amendment for cationic Cd (II), anionic As (III), roxarsone, and phosphorus in soil and water. J Cleaner Prod 247:119579. https://doi.org/10.1016/j.jclepro.2019.119579
Zhu WG, Zhu DY, He JM, Lian XX, Chang ZB, Guo RC, Li XH, Wang YL (2022) Phytoremediation of soil co-contaminated with heavy metals (HMs) and tetracyclines: effect of the co-contamination and HM bioavailability analysis. J Soils Sediments 22:2036–2047. https://doi.org/10.1007/s11368-022-03206-y